

SPECTRAL UNMIXING OF NOAA-AVHRR DATA FOR SNOW COVER ESTIMATION

N. Foppa, S. Wunderle, A. Hauser

*Remote Sensing Research Group, Departement of Geography, University of Bern,
Hallerstrasse 12, CH-3012 Bern, Switzerland
phone: ++41-31-631-80-20, fax: ++41-31-631-8511, e-mail: foppa@giub.unibe.ch*

ABSTRACT

Hydrological and climatological studies require estimates of snow-covered areas. Most such snow cover maps generated from satellite data include information of snow or not snow for each image pixel. In this study a linear spectral unmixing algorithm is used to calculate snow cover proportions within each image pixel. We examine the ability of this algorithm for operational and near-real time snow cover estimation at subpixel scale using medium spatial resolution satellite data from NOAA-AVHRR. The method presented classifies areal coverage of snow in NOAA-AVHRR 1.1 km pixel size imagery by means of unmixing the content of relatively poor spatial resolution pixels. The automated methodology is outlined which produces snow cover fraction maps showing plausible distribution of snow in comparison to a single image from the ASTER (Advanced Spaceborne Thermal Emission and Reflectance Radiometer) sensor. The qualitative analysis of the results show how suitable the approach is when implemented in the preliminary processing chain. Simplifying assumptions are made to the procedure, which explains some variation between the derived snow cover fraction map and reference data. Further work should include how accurate quantification of areal snow coverage is obtained in comparison to traditional approaches.

INTRODUCTION

Conventional classification algorithms, such as Parallelepiped or Maximum Likelihood, applied to snow cover estimation generates binary maps containing snow or not snow. Especially when using NOAA-AVHRR data on heterogeneous surfaces with small patches of snow, classified pixels contain other surface types too. Due to the relatively coarse spatial resolution of 1.1 km, each pixel area on the ground potentially contains a mixture of perhaps snow, trees, rock etc. (1, 2). To overcome this mixed pixel problem, a linear unmixing algorithm is implemented in an automated subpixel processing chain to determine the abundance of snow within each pixel.

METHODS

Linear mixture modelling considers that the signal received at the sensor is composed of a linear mixture of pure-element reflections (endmembers), where the weights are the percentage of the pixel area occupied by each element. According to (3) a general equation for mixing is:

$$DN_c = \sum_{n=1}^N F_n DN_{n,c} + E_c \quad [1]$$

where

$$\sum_{n=1}^N F_n = 1$$

and

$$0 \leq F_n \leq 1$$

with: DN_c reflectance in channel c
 N number of endmembers
 F_c fraction of endmember n
 $DN_{n,c}$ reflectance of endmember n in channel c
 E_c error in channel c of the fit of N spectral endmembers.

Equations 2 and 3 introduce the constraints that fractions sum to one and are non-negative. The system of linear equation shown above can be solved by a least square solution which minimizes the sum of squares of errors. The accuracy of the unmixing is based on E_c of equation 1, squared and summed over all M channels and could be expressed as follows:

$$\varepsilon = \sqrt{\frac{\sum_{c=1}^M E_c^2}{M}} \quad [2]$$

with ε root mean squared (rms) error
 M number of channels

A small rms error is an indication of a mathematically good model. A high rms error indicates that the model has not been constructed correctly. A certain amount of error is inevitable for different reasons. The spectral limitation of the sensor permits using only a few endmembers. There is a certain difference between image endmember and the pixel spectra, which will be unmixed due to the small number of endmembers which could only approximately describe the pixels. The residual error for each pixel is also attributed to the result of interactions of reflected light between materials. The assumptions of linear mixing models fail to take into account non-linear mixing effects between materials. Furthermore sensor noise can affect the rms error. A number of studies have shown that the linear mixing assumption is appropriate for mapping alpine snow cover at subpixel scale (2).

The maximum number of endmembers is limited by the number of spectral bands of the satellite image. Some studies, particularly for vegetation, include AVHRR thermal channels in the unmixing process, although these bands do not follow the underlying assumption of linearity because thermal emission is governed by the Planck equation which is a nonlinear function of temperature. It has been shown that the use of thermal channels does improve the results minimally and does not contribute much to the analysis of land cover (4).

The current version of the processing chain operates with the reflective channels of AVHRR/3 on NOAA-16. The newest AVHRR sensor has the advantage of a new purely reflective channel centered at 1.6 μ m (channel 3A). This provides an additional reflective channel in which snow is spectrally distinct from other materials.

PROCESSING EXAMPLE

Data are preprocessed, including calibration (5), georeferencing, atmospheric correction (6), BRDF correction (7), orthorectification and cloud masking (8). In addition water bodies are masked out. Figure 1 shows an outline of the methodology and its processing steps. The individual processing steps will be explained on the basis of a NOAA-16 dataset.

Step 1:

Identification of the purest pixels in the scene is done through compression of the data using principal component analysis (PCA) (9). The first and second PCA eigenvectors account for the majority of the variance in the data. The PCA transformation enables to extract pixels representing pure spectra from outer lines of the polygon that bounds the data space of the first two principal components (see Figure 2). This method requires no *a priori* knowledge of the image scene or spectral properties of the material within the scene. One difficulty with such an approach taken alone is that

data clouds without straight lines along the edges cannot be fitted uniquely (10). To take into account local variation of endmember spectra (11) suggests using the average spectra of several pixels from the extremes of the polygon instead of a single value.

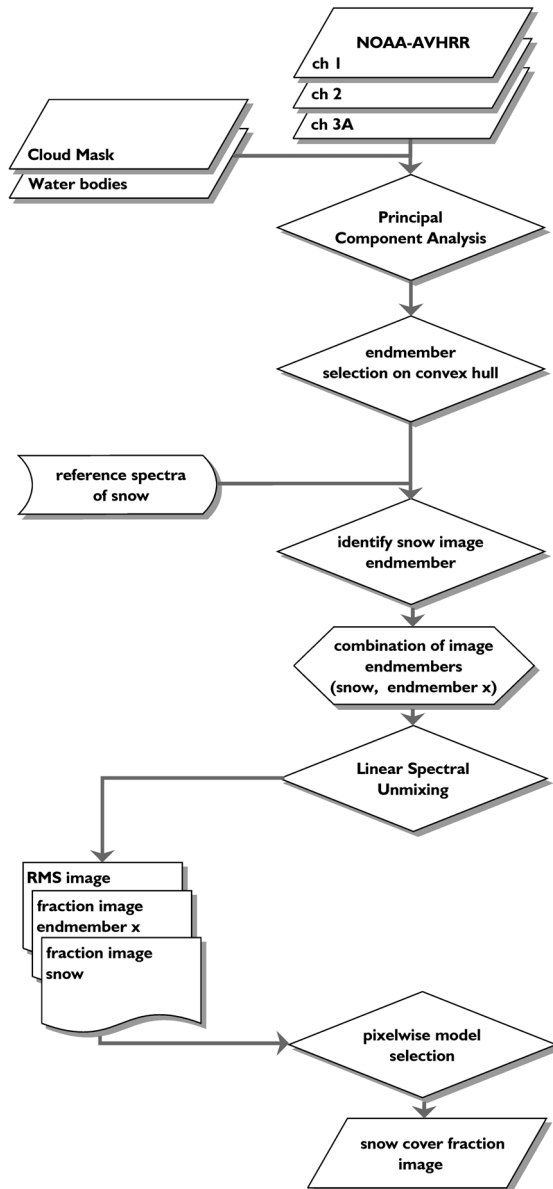


Figure 1: Flow chart of the methodology to estimate snow cover fractions from NOAA-16 AVHRR data

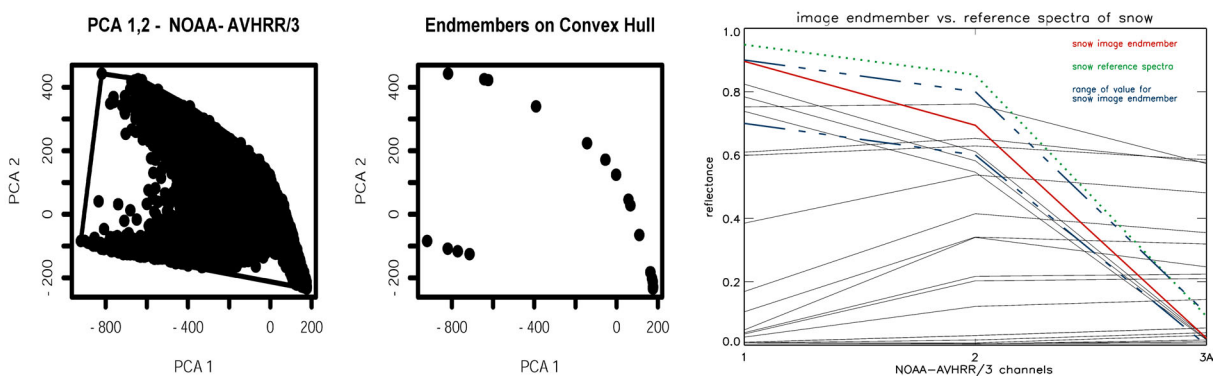


Figure 2: Endmember selection using the polygon bounding the cluster of

transformed pixels in featurespace

Figure 3: Spectral plot of identified image endmembers from convex hull

Step 2:

An arbitrarily selected range of values determines which of potential image endmembers correspond to a snow reflectance and represent a snow image endmember. The spectra next to the snow reference spectra are used as snow image endmember (see figure 3). Sets of image endmember pairs are built consisting of snow image endmember and another image endmember which is not further analysed. As seen in figure 3 several spectra lying in the mentioned range of values could refer to snow. Instead of selecting the spectra next to the reference spectra, an average of the potential snow spectra could be calculated or even each potential snow spectra could be combined with all other spectra from the convex hull. That would take into account the different reflectances of snow due to the high elevation and aspect gradients of Alpine regions resulting in a large range of the snow grain size (12).

Step 3:

In this preliminary implemented methodology it is assumed that the use of three reflective channels permits only to use two image endmembers. The image is unmixed using all endmember pairs. The output of each mixing model is composed of fraction images of the endmembers and a rms-image showing the modelling error for each pixel. The rms error is the only indicator to judge the model. As shown in equation 1 constraints are set that all the fractions should be non negative and their sum must be one. Neither the fraction overflow which outlines pixels having a fraction higher than one nor a fraction underflow with fractions less than zero is taken into account as a criterion for judging the model. Fraction overflows occur when individual pixels represent the land cover purer than the pixels used for the definition of this endmember up to now. Fraction underflows are those pixels that were not well represented by any of the endmembers.

Step 4:

The final result of the procedure is a synthesis of all computed models. The fraction of snow in each pixel corresponds to the model with the lowest rms for each pixel (Figure 4).

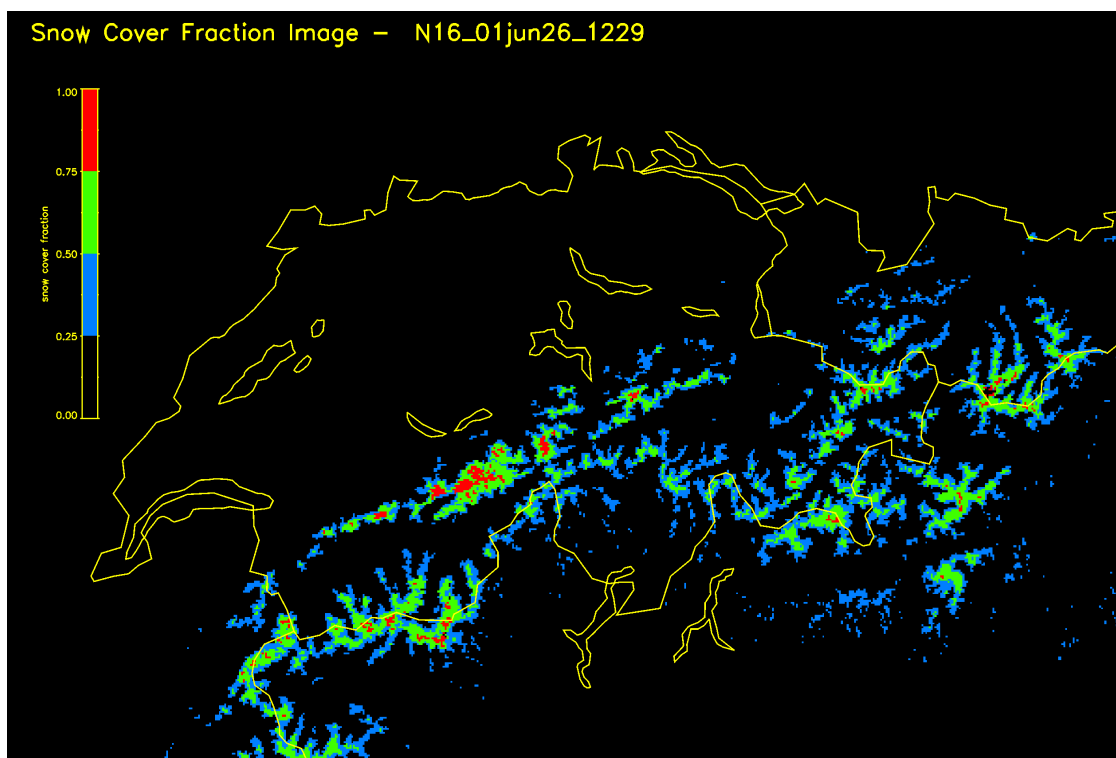


Figure 4: Snow cover proportion map as a result of different mixture models

RESULTS

The final snow cover fraction image is compared with a single image from the ASTER (Advanced Spaceborne Thermal Emission and Reflectance Radiometer) sensor on board TERRA. It should be noted that the results obtained permit only qualitative interpretation.

Visual Comparison

The visual analysis of the snow cover fraction image shows consistent distributions of snow (Figure 5, 6). The patterns of snow correspond well with reference data. Difficulties arise where clouds are not masked out and are misclassified as snow cover proportion within a pixel (see white ellipse). In contrast, pixels in mountainous areas are interpreted as being snow-free due to cloud masking.

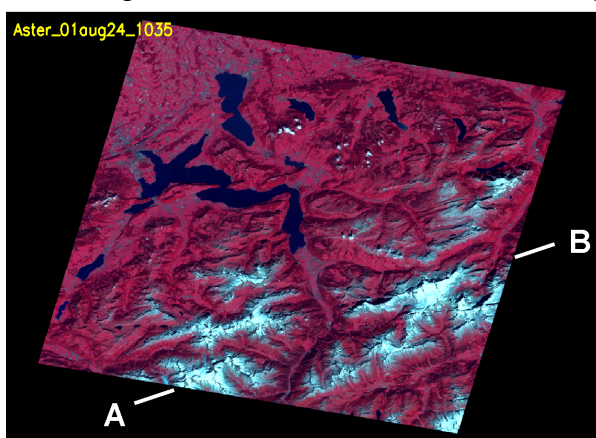


Figure 5: ASTER image of Central Switzerland

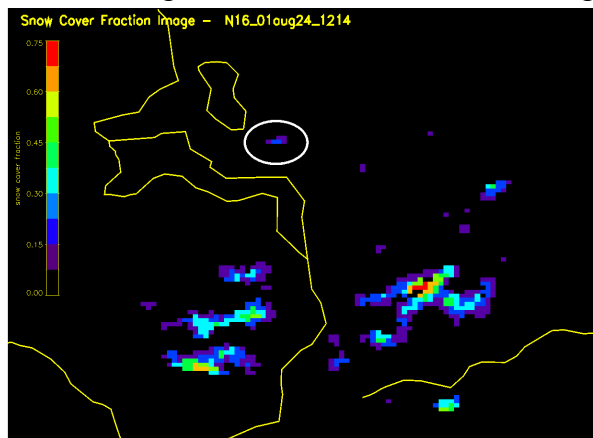


Figure 6: Snow cover proportion map from AVHRR

Transect

A synthetic snow cover fraction image at NOAA-AVHRR resolution has been calculated from unsupervised isodata classification of ASTER data and is used as reference data for validation. An arbitrarily selected transect along the image highlights the difference between NOAA-AVHRR derived snow cover fraction and the synthetic snow cover fraction image from ASTER (Figure 7). The altitude of the transect is shown by the dotted line.

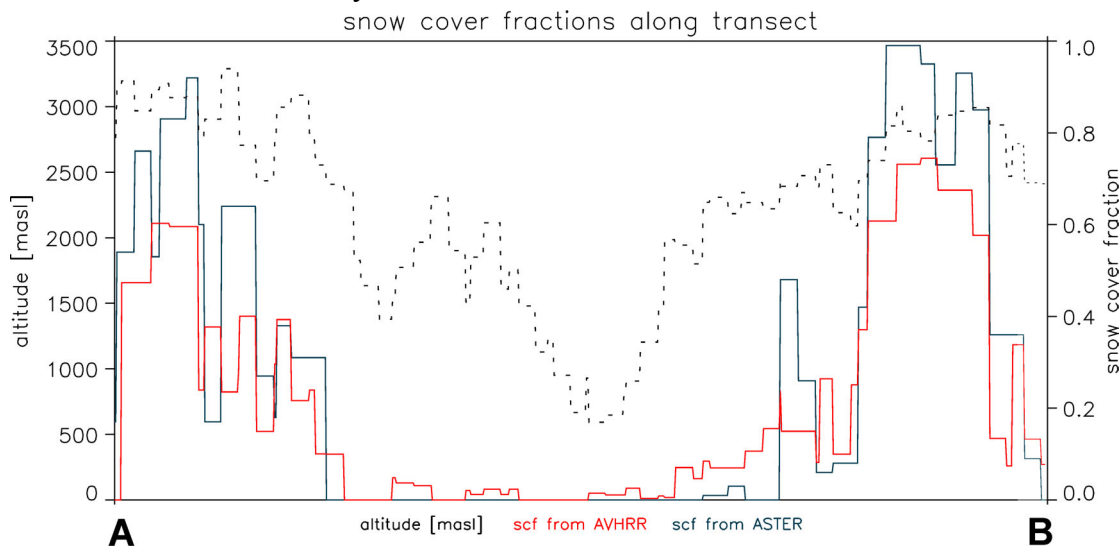


Figure 7: Snow cover fractions along a transect in the imagery for 24.08.01

The spatial profile of the snow cover map derived from the procedure presented above demonstrates the fundamental advantage of subpixel analysis aiming to overcome the problem of pixel values containing either snow or not snow. The plotted transect highlights differences between snow cover fractions. The profile from snow cover fraction calculated from AVHRR data looks quite similar to the reference profile. Some pixels comprise differences in fractions up to 0.3. Especially in the lower parts where no snow occurs during this season, snow cover fraction from AVHRR overestimates snow cover extension. From this simple comparison it can be deduced that the snow cover fraction from AVHRR suffers a tendency to underestimate snow cover in this case. It must be mentioned that the ASTER image has not been orthorectified and that a pixel to pixel comparison can suffer from coregistration.

DISCUSSION AND CONCLUSIONS

The presented procedure demonstrates the advantage of mixture modelling for snow cover estimation at subpixel resolution. The method is simple and robust and is therefore suitable for operational and near real-time applications. All steps of the processing flow are well defined and objective. It requires no human intervention, e.g. to judge the acceptability of the endmembers. Methods of manual endmember selections run the risk of finding different endmembers by different users. Simplifying assumptions are made to the endmember extraction method and to the linear unmixing algorithm due to the spectral limitation of the sensor and to ease the procedure, e.g. it is assumed that the pixels are mixtures of only two different surface cover types. These simplifications explain part of the variation of the difference between the reference data and the calculated fraction image. Different studies indicate the importance to include a shadow correction in the unmixing procedure (13, 14, 15). In the presented study variations in illumination are taken into account in the preprocessing of the data including the c-factor method which takes into account topographically induced shadow (16). The integration of an endmember with zero reflectance on all bands in mixture modelling is a possibility that is often suggested to better take into account the effects of shadow (12, 17).

Difficulties could arise if there are natural materials with very low albedo in the scene which may not be distinguishable from shade in a mixing analysis e.g. shadowed snow from bright wet soil or shallow water (2, 18).

Despite these sources of error, the snow cover proportions obtained from AVHRR compare quite well with ASTER data. An analysis of possible sources of errors must be carried out to improve the final results. Results require careful interpretation to use them as input for hydrological and climate models requiring estimates of snow-covered area. Further work should include how accurate quantification of areal snow coverage is obtained in comparison to traditional approaches.

To use the advantage of the high repetition rate of NOAA-AVHRR the processing chain must be adapted for AVHRR/2. For this sensor the reflective component of channel 3 must be estimated to produce a third reflective channel. This would make possible the comparison of snow cover fractions at different times of day derived from different AVHRR sensors.

ACKNOWLEDGEMENTS

ASTER/TERRA data was provided by the USGS EROS Data Center.

REFERENCES

1. Benham, T.B., 1998. NOAA AVHRR subpixel snow classification. M.Sc. Dissertation, University of Aberdeen.
2. Rosenthal, W. 1996. Estimating alpine snow cover with unsupervised spectral unmixing. Proceedings of IGARSS '96: 2252-2254. Lincoln, Nebraska.
3. Adams, J.B., Milton, and Gillespie, A.R. 1989. Simple models for complex natural surfaces: a strategy for the hyperspectral era remote sensing. Proceedings of IGARSS '89: 16-21. Vancouver, B.C.
4. Hlavka, C.A. and Spanner, C.A. 1995. Unmixing AVHRR imagery to assess clearcuts and forest regrowth in Oregon. IEEE Transactions on Geoscience and Remote Sensing. 33(3): 788-795.
5. ESA EPO.SHARP Level-2 User Guide, Release 1.0,1992.
6. Rahman, H. and Dedieu, G. 1994. SMAC: a simplified method for the atmospheric correction of satellite measurements in the solar spectrum. International Journal of Remote Sensing. 15(1):123-143.
7. Wu, A., Li, Z. and Cihlar, J. 1995. Effects of land cover type and greenness on advanced very high resolution radiometer bidirectional reflectances: analysis and removal. Journal of Geophysical Research. 100(5D): 9179-9192.
8. Key, J.R. The Cloud and Surface Parameter Retrieval (CASPR) System for Polar AVHRR – User's Guide, NOAA/NESDIS/ORA/ARAD/ASPT, 2001.
9. Settle, J., and Drake, N. 1993. Linear mixing and the estimation of ground cover proportions. International Journal of Remote Sensing. 14(6): 1159-1177.
10. Tompkins, S. et al. 1997. Optimization of endmembers for spectral mixture analysis. Remote Sensing of Environment. (59): 472-489.
11. Chettri, S. et al. 1997. Multi-resolution maximum entropy spectral unmixing. Proceedings of International Symposium on Artificial Intelligence, Robotics and Automatisation in Space '97: 347-352. Tokyo.
12. Painter, T.H. et al. 1998: The effect of grain size on spectral mixture analysis of snow-covered area from AVIRIS data. Remote Sensing of Environment. (65): 320-332.

13. Asner, G.P., Wessman, C.A., Privette, J.L. 1997. Unmixing the directional reflectances of AVHRR sub-pixel landcovers. *IEEE Transactions on Geoscience and Remote Sensing*, 35(4): 868-878.
14. Adams, J.B. et al., 1995: Classification of multispectral images based on fractions of endmembers: applications to land-cover change in the Brazilian Amazon. *Remote Sensing of Environment*. (52): 137-154.
15. Solberg, R., Vikhamar, D. 2000. A method for optical snow-cover mapping in sparse forest. *Proceedings of IGARSS '00, IEEE International Geoscience and Remote Sensing Symposium, Hawaii, USA*. 1769-1771.
16. Teillet, P.M. and Holben, B.N. 1982. On the slope-aspect correction of multispectral scanner data. *Canadian Journal of Remote Sensing*. 8(2):84-106.
17. Hill, J. Mehl, W., Altherr, M. 1994. Land degradation and soil erosion mapping in a Mediterranean ecosystem. *Imaging Spectrometry – a Tool for Environmental Observations*, edited by Hill J. and Mégier J. (Brussels and Luxembourg), 237-260.
18. Blount, G. et al. 1990. Regional aeolian dynamics and sand mixing in the Gran Desierto: evidence from Landsat Thematic Mapper images. *Journal of Geophysical Research*. 95(15): 463-15,482.